LAWRENCE
LIVERMORE
NATIONAL
LABORATORY

LLNL-JRNL-420984

Symmetric inertial confinement fusion implosions at ultra-high laser energies

S. H. Glenzer, B. J. MacGowan, P. Michel, N. B. Meezan, L. J. Suter, S. N. Dixit, J. L. Kline, G. A. Kyrala, D. A. Callahan, E. L. Dewald, L. Divol, E. Dzenitis, J. Edwards, A. V. Hamza, C. A. Haynam, D. E. Hinkel, D. H. Kalantar, J. D. Kilkenny, O. L. Landen, J. D. Lindle, S. LePape, J. D. Moody, A. Nikroo, T. Parham, M. B. Schneider, R. P. J. Town, P. Wegner, K. Widmann, P. Whitman, B. K. F. Young, B. Van Wonterghem, J. E. Atherton, E. I. Moses

December 4, 2009

Science

Disclaimer

Symmetric inertial confinement fusion implosions at ultra-high laser energies

S. H. Glenzer, B. J. MacGowan, P. Michel, N. B. Meezan, L. J. Suter, S. N. Dixit, J. L. Kline[2], G. A. Kyrala[2], D. A. Callahan, E. L. Dewald, L. Divol, E. Dzenitis, J. Edwards, A. V. Hamza, C. A. Haynam, D. E. Hinkel, D. H. Kalantar, J. D. Kilkenny[3], O. L. Landen, J. D. Lindl, S. LePape, J. D. Moody, A. Nikroo[3], T. Parham, M. B. Schneider, R. P. J. Town, P. Wegner, K. Widmann, P. Whitman, B. K. F. Young, B. Van Wonterghem, J. E. Atherton, E. I. Moses

[1]Lawrence Livermore National Laboratory, P.O. Box 808, Livermore, CA 94551, USA. [2]Los Alamos National Laboratory, Los Alamos, New Mexico 87545, [3]General Atomics, San Diego, CA [†]Corresponding author; glenzer1@llnl.gov

The first indirect-drive hohlraum experiments at the National Ignition Facility have demonstrated symmetric capsule implosions at unprecedented laser drive energies of 0.7 MJ. 192 simultaneously fired laser beams heat ignition hohlraums to radiation temperatures of 3.3 million Kelvin compressing 1.8-millimeter capsules by the soft x rays produced by the hohlraum. Self-generated plasma-optics gratings on either end of the hohlraum tune the laser power distribution in the hohlraum producing symmetric x-ray drive as inferred from capsule self-emission measurements. These experiments indicate conditions suitable for compressing deuterium-tritium filled capsules with the goal to achieve burning fusion plasmas and energy gain in the laboratory.

With completion (1) and commissioning (2) of the National Ignition Facility (NIF) at the Lawrence Livermore National Laboratory the quest for producing a burning fusion plasma has begun (3,4). The goal of these experiments is to compress matter to densities and temperatures higher than the interior of the sun (5-7) which will initiate nuclear fusion and burn of hydrogen isotopes (8-10). This technique holds promise to demonstrate a highly efficient carbon–free process that will burn milligram quantities of nuclear fuel on each laser shot for producing energy gain in the laboratory.

The NIF consists of 192 laser beams that have been arranged into cones of beams to irradiate a target from the top and bottom hemispheres. This "indirect-drive" laser geometry has been chosen for the first experiments to heat the interior of centimeter-scale cylindrical gold hohlraums (8,11-14) through Laser Entrance Holes (LEH) on the top and bottom end of the cylinder (Fig. 1). Hohlraums act as radiation enclosures that convert the optical laser light into soft x-rays that are characterized by the radiation temperature T_{RAD}. Present ignition designs operate at temperatures of 270 to 305 eV or 3.1 to 3.5 million K. The radiation field compresses a spherical fusion capsule mounted in the center of the hohlraum by x-ray ablation of the outer shell. The ablation process compresses the cryogenically prepared solid deuterium-tritium fuel layer in a spherical rocket implosion. In the final stages, the fuel reaches densities 1000-times solid and the central hot spot temperatures will approach 100 million K to initiate the nuclear burn process.

In experiments at the NIF, we have symmetrically imploded 1.8-mm diameter fusion capsules in cryogenically fielded centimeter-scale hohlraums at 20 K. These experiments are performed with more than 20 times higher laser energy than previously delivered (11-14) and show efficient hohlraum heating to radiation temperatures of 3.3 million K. In addition, the large scale-length plasmas encountered in these experiments have allowed us to employ, for the first time, self-generated plasma optics gratings (15) to fully control the radiation symmetry (16) and to achieve symmetric fusion capsule implosions.

Figure 2 (a) shows the laser power at the frequency-tripled wavelength of 351 nm versus time for two different pulse shapes used in this study. These 11-ns and 16-ns long pulses heat 8.6-mm long, 4.6-mm diameter hohlraums with 20% helium, 80% hydrogen (atomic) mixtures and 100% helium gas fill, respectively. The laser peak powers of P_L = 220 TW and 245 TW have been distributed initially among the inner beams at 23.5˚ and 30˚ and the outer beams at 44.5˚ and 50˚ with a ratio of 1:2 as required for a symmetric implosion.

These hohlraums absorb more than 90% of the laser energy. Losses are due to laser back scattering by Stimulated Raman Scattering (SRS) on the inner beams (17,18). Stimulated Brilllouin scattering and SRS on outer beams is negligible for our conditions. The inner beams interact with capsule and hohlraum wall blow-off plasma where radiation-hydrodynamic simulations (19) and laser-plasma interaction calculations (20) show amplification gains for SRS of 10-20. We observe SRS in the wavelength range from 500-650 nm that is measured spectrally and temporally resolved on two quads of beams on the 30˚ and the 50˚ cone. The SRS signal propagating back into the focusing lens is transmitted through the final turning mirror and measured with a full aperture backscatter station (21). In addition, light scattered from the hohlraum around the final optics is reflected by an absolutely calibrated scatter plate and measured with gated CCD cameras (22). The experiments show that 21% and 15% of the incident inner beam energy is reflected at the time around peak laser intensity, c.f., Fig. 2(a). Since back scattering on the outer beams is negligible, these measurements show that hohlraums with helium-hydrogen gas mixtures absorb 93% of the laser energy while hohlraums filled with helium gas show a total absorption of 95%.

With η_{ce} being the conversion efficiency from laser power, P_L, to soft x-rays, the hohlraum radiation temperature is determined by balancing the absorbed laser power with the x-ray power radiated into the wall, P_W, absorbed by the capsule, P_{CAP}, and the power that escapes though the LEH, P_{LEH},

$$\begin{aligned}\eta_{CE}(P_L - P_{Backscatter}) &= P_W + P_{LEH} + P_{CAP} \\ &= \sigma T_{RAD}^4[(1-\alpha_W)A_W + A_{LEH} + (1-\alpha_{CAP})A_{CAP}].\end{aligned} \quad (1)$$

Here, σ denotes the Stefan-Boltzmann constant; α_W and α_{CAP} are the albedo of the hohlraum wall and the capsule. The albedo is defined as the fraction of re-emitted over incident x-rays. Further, A_W, A_{LEH}, and A_{CAP} are the hohlraum wall area, laser entrance hole area, and capsule surface area, respectively. Assuming a conversion efficiency of η_{ce} = 0.9 at peak laser power, Eq. (1) indicates peak radiation temperatures of 260 eV < T_{RAD} < 280 eV.

Figure 2(b) shows the radiation temperature inferred from the measured total x-ray hohlraum emission and from detailed radiation-hydrodynamic simulations using the code LASNEX (19). An absolutely calibrated broadband x-ray spectrometer, Dante, measures the x-ray flux emitted from the LEH in the energy range of 0 < $E_{X\text{-}ray}$ < 20 keV (23). The x-ray power in the direction of Dante in units of GW/sr is determined by $dP/d\Omega = A_{LEH}(t)\cos\theta\ \sigma T_{PAA}^4/\pi$, where θ is the view angle of Dante towards the hohlraum axis. To determine T_{RAD}, we infer the dynamically varying source area, $A_{LEH}(t)$, from 3-5 keV x-ray pinhole camera images of

the LEH. The experiments reach peak radiation temperatures of 285 eV after going through three low-power steps that drive coalescing shocks in ignition capsules. The experimental data are in excellent agreement with the radiation hydrodynamic modeling at all times, and further agree with the estimate provided by Eq. (1). The calculations indicate peak ablation pressures of 120 to 142 Mbar resulting in a capsule convergence of 10-15 in radius and in a compressed capsule inner shell diameter of 100 μm.

Figure 3 (a) shows capsule implosion images at time of peak emission that occurs 1-2 ns after the end of the laser drive. These measurements show the x-ray self-emission at 9 keV energy observed through an 500 μm diagnostic window in the side of the hohlraum. The images are taken using a pinhole array with 15x magnification and a gated microchannelplate detector that yields temporal resolution of 80 ps. The capsules have been filled initially with a high-pressure gas mixture of 90% helium and 10% deuterium at 2594 torr (at 20 K). Thus, convergence is limited to a capsule x-ray emission radius of 50 μm with central ion temperatures in excess of T_i = 30 million K as inferred from the D-D neutron time of flight spectrum. At these temperatures and densities, the capsule self-emission provides a sensitive measure of the hohlraum soft x-ray drive symmetry (24,25).

Figure 3 shows that the capsule symmetry is controlled by the laser wavelength choice on the inner and outer cone of beams. In particular, a wavelength difference of Δλ=1.7Å results in excellent implosion symmetry as required for ignition experiments. On the other hand, at Δλ=0.5Å, we observe an oblate implosion shape indicating a locally reduced x-ray drive in the hohlraum equatorial plane.

These observations can be quantified by decomposing the soft x-ray flux asymmetry at the capsule into Legendre polynomials, P_n. Odd orders (n = 1,3,…) are approximately zero due to the up-down illumination symmetry and low-order even modes (n = 2, 4) are the most important asymmetries. Higher order drive variations are negligibly small and smoothed by the hohlraum radiation environment. While small wavelength differences result in oblate implosions, P_2/P_0 = -0.42 at Δλ=0.5Å and P_2/P_0 = -0.24 at Δλ=1Å, we obtain a symmetric implosion for sufficiently large shifts, i.e., P_2/P_0 = 0.02 at Δλ=1.7Å. For all cases, we find $P_4/P_0 = 0.09 \pm 0.02$ (here, P_0 = 50 μm denotes the radius of the imploded core).

We achieve symmetric implosions and adequate equatorial x-ray drive without changing the initial inner and outer cone laser powers. This tuning mechanism takes advantage of the multiple laser beam interactions (26,27) with the plasma in the LEH area where all the beams cross. Transferring power into the inner beams, allows us to compensate for SRS losses of the inner beams. Although inner beam SRS energy losses of 5 to 7 % are energetically small not significantly affecting radiation temperatures, these losses may affect the local soft x-ray production.

As shown in the inset of Fig. 1, and indicated by the interference fringes, the crossing laser speckles in the LEH produce spatial intensity modulations. These intensity modulations further drive plasma electron density modulations due to the ponderomotive force. If these modulations move with the plasma sound speed C_S (in the frame of the plasma), modulations and laser scattering will grow to larges levels and efficient energy transfer between beams will occur. In the rest frame, the power transfer rate, Q, is determined by

$$Q \sim \left[(\omega_1 - \omega_2) - k_A(C_S - V) + i\nu\right]^{-2}. \qquad (2)$$

In Eq. (2), V is the plasma flow velocity and $i\nu$ is the Landau damping rate for acoustic fluctuations. The frequency de-tuning between pairs of beams is denoted as $\omega_1 - \omega_2$. This factor allows us to control the energy transfer between cones of beams in integrated hohlraum experiments, and can be set to transfer power into either cone of beams. Proper choice of the laser wavelengths is therefore required to obtain the desired x-ray drive symmetry.

Figure 3 (b) shows a linear dependence of P_2/P_0 on the wavelength tuning difference Δλ. This fact has allowed us to tune the implosion symmetry in three shots. This observation has been expected for the small tuning range (16) and constant SRS levels in this study. A linear scaling further agrees with power-transfer calculations that include the detailed calculated plasma conditions and flow profiles in the LEH region. Although the experimental scaling is reproduced, the P_2 zero crossing is not accurately calculated. A difference of 0.5Å can be explained by, e.g., errors of order 10% in the calculated plasma flow profile

Moreover, best agreement is observed when including a model that assumes enhanced inner beam laser beam absorption in the low-Z plasma. This assumption is motivated by observations of increasing levels of hot electrons at the peak of the laser drive with increasing wavelength shift. The hot electron fraction reaches levels between 1-2% of the laser energy indicating finite levels of re-absorbed SRS in the hohlraum. Without the absorption model the calculated slope increases by 20%.

In summary, we have demonstrated efficient laser coupling and symmetric capsule implosions in cryogenic hohlraum experiments on the National Ignition Facility. These experiments meet simultaneous requirements on laser coupling and symmetry for future ignition shots. The measured insensitivity of SRS losses to the power level of the inner cone beams will motivate future higher radiation-temperature experiments with larger laser intensities and energies.

References and Notes

1. E. Moses, C. R. Wuest, Fusion Sci. Tech. **47**, 314 (2005).
2. C. Haynam et al., Appl. Optics **46** 3276 (2007).
3. D. Clery, Science **324**, 326 (2009).
4. J. Nuckolls, L. Wood, A. Thiessen, G. Zimmerman, Nature **239**, 139 (1972).
5. R. P. Drake, High-Energy-Density Physics (Springer, New York, 2006). B. A. Remington, R. P. Drake, D. D. Ryutov, Rev. Mod. Phys. **78**, 755 (2006).
6. R. A. García et al., Science **316** 1591 (2007).
7. D. O. Gough et al., Science **272**, 1296 (1996).
8. J. D. Lindl *et al.,* Phys. Plasmas **11**, 339. (2004).
9. S. Atzeni, J. Meyer-ter-Vehn, The Physics of Inertial Fusion (Oxford Univ. Press, New York, 2004).
10. R. L. McCrory *et al.,* Phys. Plasmas **5**, 055503 (2008).
11. L. J. Suter *et al.,* Phys. Rev. Lett. **73**, 2328 (1994).
12. R. L. Kauffman *et al.,* Phys. Rev. Lett. **73**, 2320 (1994).
13. W. J. Krauser, Phys. Plasmas **3**, 2084 (1996).
14. S. H. Glenzer et al., Phys. Rev. Lett. **80**, 2845 (1998).
15. W. L. Kruer et al., Phys. Plasmas **3**, 382 (1996). W. L. Kruer, *The Physics of Laser Plasma Interactions* (Addison-Wesley, New York, 1988).
16. P. Michel et al., Phys. Rev. Lett. **102**, 025004 (2009). P. Michel et al., Phys. Plasmas **16**, 024702 (2009).
17. B. J. MacGowan et al., Phys. Plasmas **3**, 2029 (1996).
18. J. C. Fernandez et al., Phys. Plasmas **4**, 1849 (1997).
19. G. B. Zimmerman and W. L. Kruer, Comments Plasma Phys. Control. Fusion **2**, 85 (1975).
20. R. L. Berger et al., Phys. Plasmas **5**, 4337 - 4356(1998).
21. D. H. Froula et al., Rev. Sci. Instrum. **75**, 4168-4171 (2004).
22. A. J. Mackinnon et al., Rev. Sci. Instrum. **75**, 4183-4186 (2004).
23. E. L. Dewald et al., Rev. Sci. Instrum. **75**, (2004).
24. A. A. Hauer *et al.,* Phys. Plasmas **2**, 2488 (1995).
25. O. L. Landen *et al.,* Phys. Plasmas **6**, 2488 (1999).
26. K. B. Wharton et al., Phys. Rev. Lett. **81**, 2248 (1998).
27. R. K. Kirkwood et al., Phys. Rev. Lett. **89**, 215003 (2002).

28. This work was performed under the auspices of the U.S. Department of Energy by Lawrence Livermore National Laboratory under Contract DE-AC52-07NA27344.

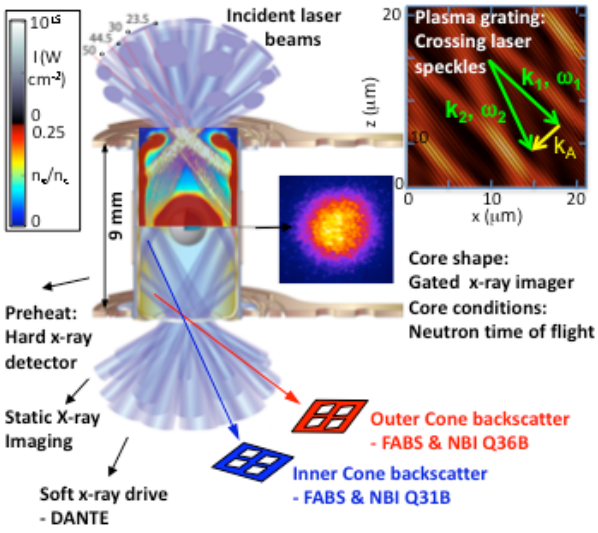

Fig. 1: Schematic of experimental setup. Hohlraums (8.6 mm long, 4.6 mm diameter, 2.9 mm LEH) that are scaled in size to 78% of a full ignition target are irradiated by 192 high-power laser beams. The beams are arranged in 4 cones of beams, the beams at 23.5˚ and 30˚ to the hohlraum axis comprise the inner beams and beams at 44.5˚ and 50˚ to the axis are the outer beams. The wavelength of the outer beams can be tuned with respect to the inner beams to control the laser power distribution inside the hohlraum by scattering laser light on a plasma grating in the beam crossing area. An example of the calculated laser intensity in the hohlraum is shown with a black and white color bar reaching peak intensities of 10^{15} W cm^{-2}. The lasers heat and ionize the hohlraum gas fill on their way to the walls forming a high-temperature low-density plasma inside the hohlraum. The density contour shows the electron density normalized to the critical density indicating tamping of the capsule and hohlraum wall blow off. Laser coupling, x-ray production and capsule implosion conditions are measured with a suite of optical, x-ray, and neutron detectors.

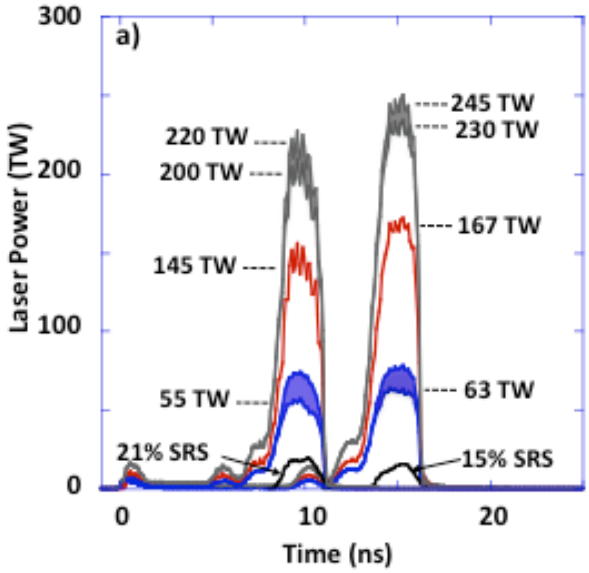

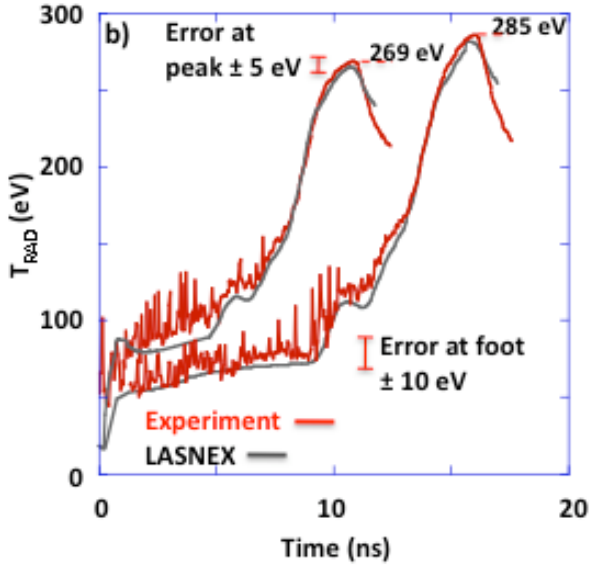

Fig. 2: (A) Total laser powers are shown together with power on the outer cone, inner cone, and the reflected SRS power on the inner cone. For the 11-ns, 568 kJ pulses, the laser delivers peak powers of 220 TW. SRS losses, indicated as shaded areas, reduce the hohlraum absorbed peak power to 200 TW. For the 16-ns, 664 kJ pulses, the laser delivers peak powers of 245 TW with 230 TW peak absorbed power in the hohlraum. (B) The hohlraums heat to peak radiation temperatures of 269-285 eV in close agreement with radiation-hydrodynamic modeling. The error bar is calculated from uncertainties of the absolute detector calibration and from uncertainties of the LEH area and soft x-ray background signals.

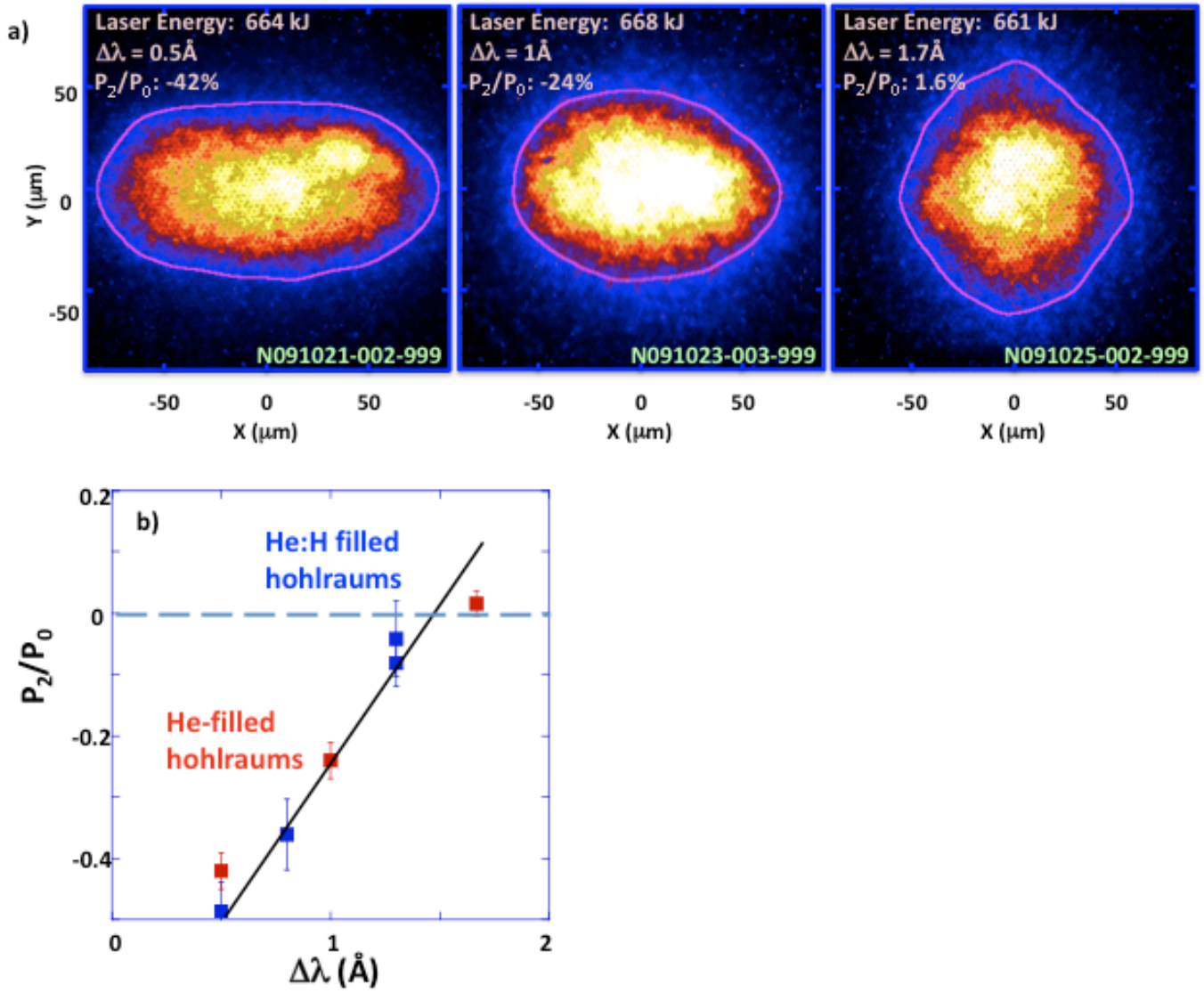

Fig. 3: (A) Capsule x-ray emission images at 9-keV energy from helium-filled hohlraums are shown as function of the wavelength difference between the laser beams on the inner and outer cones. The axis of symmetry is vertical. (B) The low-order even Legendre polynomial is shown for two different hohlraum conditions and laser pulse shapes indicating a linear scaling in agreement with the calculations. The error bar is estimated from determining the Legendre polynomial from multiple simultaneously measured images. The dashed curve indicates a symmetric implosion and the solid curve is the scaling calculated from two-dimensional radiation hydrodynamic simulations.